PHILOSOPHICAL TRANSACTIONS A

rsta.royalsocietypublishing.org

Research

Cite this article: Luk'yanchuk B, Paniagua-Domínguez R, Kuznetsov AI, Miroshnichenko AE, Kivshar YS. 2017 Suppression of scattering for small dielectric particles: anapole mode and invisibility. *Phil. Trans. R. Soc. A* **375**: 20160069. http://dx.doi.org/10.1098/rsta.2016.0069

Accepted: 5 September 2016

One contribution of 16 to a theme issue 'New horizons in nanophotonics'.

Subject Areas:
optics

Keywords:
high-index dielectric nanoparticles, Mie resonances, toroidal mode, anapole

Author for correspondence:
Boris Luk'yanchuk
e-mail: boris_l@dsi.a-star.edu.sg

Suppression of scattering for small dielectric particles: anapole mode and invisibility

Boris Luk'yanchuk[1,2], Ramón Paniagua-Domínguez[1], Arseniy I. Kuznetsov[1], Andrey E. Miroshnichenko[3] and Yuri S. Kivshar[3]

[1]Data Storage Institute, A*STAR (Agency for Science, Technology and Research), 2 Fusionopolis Way, 08-01 Innovis, 138634 Singapore
[2]Division of Physics and Applied Physics, School of Physical and Mathematical Sciences, Nanyang Technological University, 637371 Singapore
[3]Nonlinear Physics Centre, Research School of Science and Engineering, The Australian National University, Acton, Australian Capital Territory 2601, Australia

BL, 0000-0001-8050-7212

We reveal that an isotropic, homogeneous, subwavelength particle with high refractive index can produce ultra-small total scattering. This effect, which follows from the inhibition of the electric dipole radiation, can be identified as a Fano resonance in the scattering efficiency and is associated with the excitation of an anapole mode in the particle. This anapole mode is non-radiative and emerges from the destructive interference of electric and toroidal dipoles. The invisibility effect could be useful for the design of highly transparent optical materials.

This article is part of the themed issue 'New horizons in nanophotonics'.

1. Introduction

The idea of perfect camouflage follows the history of mankind. This idea has inspired poets and writers, who described the great advantages that invisibility could bring for military or political purposes or even love affairs. In this context, the stories from *The Thousand and One Nights* (also called *The Arabian Nights*), Alexander Pushkin's poem *Ruslan and Ludmila*, or novels such as *The Invisible Man* by H. G. Wells or J. K. Rowling's character Harry Potter can be mentioned among many others. For a

THE ROYAL SOCIETY PUBLISHING

long time, invisibility was considered to be forbidden by general physics. Since the times of Rayleigh [1,2], it has been widely accepted that even a very small particle will be visible due to light scattering. Attempts to realize invisibility were based on camouflage (i.e. imitating the colour of the background, in the way chameleons do) and, thus, just palliative.

In his book, published in 1962 (English translation published in 1971 [3]), P. Y. Ufimtsev suggested another principle to realize invisibility. The idea, aimed at making an aircraft invisible to radars, was to use a geometrical shape that would minimize its backscattering. Such a configuration can be easily implemented, for example, with a conical mirror directed towards the light source. It is interesting to note that Prof. M. Levin (who was a referee of Ufimtsev's Doctoral thesis) wrote in his official review that zero backscattering could be obtained for an azimuthally symmetric body provided the constituent material had equal electric permittivity and magnetic permeability, i.e. $\varepsilon = \mu$. Ufimtsev highlighted this story in his book [4], but it was never published in the form of a paper. Afterwards, the same idea was independently discovered [5] and published by M. Kerker, in the context of scattering from magnetic spheres. Following this publication, the condition $\varepsilon = \mu$ is commonly known as the first Kerker condition. Kerker further developed the idea of achieving total scattering suppression. For that, he considered the scattering from multi-layered spheres [6] and spheroids [7].

A step further in the development of the invisibility idea was taken with the development of the concept of cloaking [8,9], which uses the general principle of optical transformation, i.e. Fermat's principle. The first attempts to realize the cloaking concept involved inhomogeneous media with some very special profiles of permittivity $\varepsilon = \varepsilon(\mathbf{r})$ and permeability $\mu = \mu(\mathbf{r})$ that were necessary to 'guide' light around the cloaking area and thus were not very practical. Other ideas related to multi-shell structures for cloaking based on plasmonic [10], dielectric [11] and metamaterial coatings have also been developed along with scattering cancellation and mantle cloaking concepts [12].

Coming back to the homogeneous sphere case, one should mention the concept of directional scattering, first predicted at optical frequencies for plasmonic nanoparticles. This idea is closely related to Fano resonances in plasmonic materials and metamaterials [13,14] and may lead to scattering minimization in a given direction, including backwards. However, in general, these effects are not accompanied by a minimization of the total scattering efficiency and, therefore, the particle is perfectly visible from any other direction. Another problem is related to dissipation of lightwave energy in real metals, which causes light extinction and makes the particle visible. This issue can be circumvented if dielectric particles are used instead.

2. Rayleigh approximation

The scattering efficiency, Q_{sca}, in the Rayleigh scattering regime is given by the well-known formula [15]

$$Q_{\mathrm{sca}}^{(Ra)} = \frac{8}{3}\left(\frac{\varepsilon - 1}{\varepsilon + 2}\right)^2 q^4, \tag{2.1}$$

which represents the ratio of the scattering cross section to the geometrical one, $\sigma_{\mathrm{geom}} = \pi R^2$, where R is the particle radius, ε is its permittivity and $q = 2\pi R/\lambda$ is the size parameter, with λ the radiation wavelength. The particle is considered to be an ideal sphere made of an isotropic, homogeneous and non-magnetic ($\mu = 1$) material. In addition, the size of this particle should be small enough so that the dipolar approximation holds. If one considers non-dissipative, $\mathrm{Im}\varepsilon = 0$, dielectric materials with a positive refractive index $n = \sqrt{\varepsilon} > 1$, then the ratio of scattering efficiency to the fourth power of the size parameter follows a universal function, which monotonously increases with refractive index as

$$\frac{Q_{\mathrm{sca}}^{(Ra)}}{q^4} = \frac{8}{3}\left(\frac{n^2 - 1}{n^2 + 2}\right)^2. \tag{2.2}$$

Equations (2.1) and (2.2) describe the scattering of an electric dipole and can be derived from Mie theory [15], which is the exact solution of plane wave scattering from a spherical particle. The

scattering efficiency of the particle, according to Mie theory, is given by

$$Q_{\mathrm{sca}} = \frac{2}{q^2}\sum_{\ell=1}^{\infty}(2\ell+1)[|a_\ell|^2 + |b_\ell|^2], \tag{2.3}$$

where the scattering amplitudes a_ℓ (electric) and b_ℓ (magnetic) are expressed in terms of the Riccatti–Bessel functions [15]. With small size parameter, $q \ll 1$, one can find [16] that $a_\ell \propto q^{2\ell+1}$ and $b_\ell \propto q^{2\ell+3}$. Therefore, for a small particle, the electric dipole amplitude a_1 is dominant.

Let us start by considering a small, plasmonic particle with $\varepsilon < 0$. It can be seen that, under some circumstances, the scattering efficiency can be very large, $Q_{\mathrm{sca}} \gg 1$. The physical reason for this effect can be explained from the Poynting vector's field [16,17], from which it can be seen that the particle may capture energy from an area that greatly exceeds its geometrical cross section. This situation holds, for example, near plasmonic resonances, excited when the condition $\varepsilon = -(1+\ell^{-1})$ is approximately fulfilled. Note that, at resonance, the Rayleigh approximation is not valid. As an example, $Q_{\mathrm{sca}}^{(Ra)}$ in formula (2.1) has singularity when $\varepsilon = -2$ (which leads to the excitation of the electric dipole resonance). On the contrary, Mie theory yields a perfectly defined and finite value of $Q_{\mathrm{sca}} = 6/q^2$ at this resonance. Interestingly, for weakly dissipative plasmonic materials, an inversion of the hierarchy of resonances may be observed. In this situation, the scattering efficiency at the dipole resonance can be smaller than that of the quadrupole one, which can be, in turn, smaller than that for the octupole resonance, etc. [18].

If a small dielectric particle with $\varepsilon > 1$ is considered instead, the Rayleigh approximation (2.1) shows that it produces a very small scattering, which tends to zero as $q \to 0$. This limit corresponds to the situation in which the electric dipole amplitude plays a dominant role and all other amplitudes are small. Such a situation is typical for particles with a small size parameter $q \ll 1$ and a refractive index $1 < n < 2$ [19]. In this case, the Rayleigh formula (2.1) represents the minimal possible scattering of a small particle.

3. High-index dielectric particles

The situation changes for a particle with high refractive index. Silicon (Si) particles at optical frequencies ($n \approx 4$) have resonant scattering efficiencies with an inverted hierarchy. For example, at the magnetic dipole resonance, the scattering efficiency is larger than that at the electric dipole resonance, even for small particles [20,21]. This has been experimentally confirmed [22,23]. As a result, in spite of fulfilling the condition that the particle size is small, the scattering near the resonances is not small. This follows from the fact that, actually, the true conditions for the applicability of formula (2.1) are $q \ll 1$ and, additionally, $q < 1/n$. This is easy to see in figure 1*a*, where the total Mie scattering and Rayleigh scattering efficiencies as a function of refractive index n are presented for a spherical particle with size parameter $q = 0.3$ ($R/\lambda \approx 0.05$). Rayleigh scattering saturates at large n, but equation (2.1) loses its validity in the vicinity of the magnetic dipole resonance at $n = 10.3$ and also in the vicinity of the subsequent resonances (as shown in the inset of figure 1*a*). Note that some very narrow peaks cannot be seen on the scale of this inset. Also note that, even with a large refractive index, the total scattering between resonances is quite close to Rayleigh scattering (blue line).

It is not surprising that the particle has a scattering efficiency much larger than Rayleigh scattering near resonances. However, the asymmetric line-shape of the resonance (figure 1*a*) leads also to a strong suppression of the total scattering near the resonance that becomes lower than that given by the Rayleigh formula (2.1). This effect is observed, for example, in the region near $n \approx 15$, denoted by a dashed box in figure 1*a*. A zoom into this area is shown in figure 1*b*. In this figure, it can be seen that there are two closely situated electric dipole and magnetic quadrupole resonances, which could not be resolved on the scale of figure 1*a*. Although there are many points with local scattering minima, as shown in the inset to figure 1*a*, a more precise examination shows that the global minimum in scattering is reached at the minimum of the resonance near $n \approx 15$. The total scattering efficiency, $Q_{\mathrm{sca}} \approx 5.99 \times 10^{-3}$, for this particle is about 3.5 times smaller than

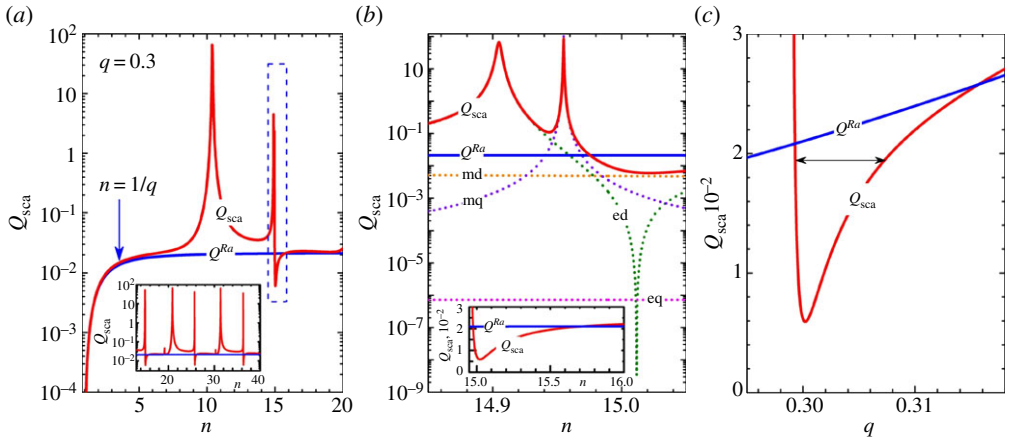

Figure 1. (*a*) Scattering efficiencies of a spherical particle according to the Rayleigh approximation (blue line) and exact Mie theory (red line) for small size parameter $q = 0.3$. The inset in (*a*) shows resonances at higher values of the refractive index. In the vicinity of $n \approx 15, 26, 36 \ldots$ one can see that the total scattering is less than the value from equation (2.1). A zoom of the scattering within the area indicated by the dashed box is shown in (*b*), where the Rayleigh approximation (blue line) and exact Mie theory (red line) are shown together with four partial scattering efficiencies for magnetic dipole (md), electric dipole (ed), magnetic quadrupole (md) and electric quadrupole (eq). Inset in (*b*) shows the $Q_{sca} < Q^{Ra}$ region versus the refractive index. (*c*) The $Q_{sca} < Q^{Ra}$ region versus the size parameter.

the Rayleigh scattering, calculated with formula (2.1), $Q_{sca}^{(Ra)} \approx 2.11 \times 10^{-2}$. A detailed analysis of this resonance reveals that it has a typical Fano shape, with a narrow bandwidth, as depicted in figure 1*c*.

Previously, it was shown that such a Fano shape arises in the total scattering from single elongated antennas, both in the plasmonic case [24,25] and in their dielectric analogues [26], within a system of disordered photonic crystals [27] as well as in the transmission spectra of a two-dimensional square lattice of dielectric circular rods [28]. In the last case, the Fano resonance arises due to the interplay between the resonant Mie scattering from individual rods and the Bragg scattering from the photonic lattice. Another example of the Fano profile is observed in the dipole scattering amplitude $|a_1(n)|^2$ of an infinite cylinder in the limit $n \gg 1$ [29]. Formally, the results of Tribelsky & Miroshnichenko [29] can be expressed as an interference of two partitions, one corresponding to the n-independent wave scattered by a perfectly reflecting particle and playing the role of the background in the Fano mechanism, and the other associated with the excitation of an n-dependent, resonant Mie mode [30].

In our case, the Fano shape is associated with the destructive interference of an electric dipole mode with a toroidal dipole mode. Previously, it was shown that such a type of interference, the so-called anapole mode [31,32], could be observed in Si nanodiscs. For nanodiscs, this anapole mode can be achieved at a specific wavelength and for some fixed ratio of the disc height to its diameter. It was shown that in the case of a single, isolated, non-magnetic, isotropic, spherical particle the anapole condition is usually hidden by the rest of the multi-polar contributions. Here, we show that the anapole excitation may be observed even in the simple spherical case, provided the particle is sufficiently small and has a sufficiently high refractive index. In figure 2, we present the Poynting vector distribution for the particle with $n = 15.01$ and $q = 0.3$, showing a clear toroidal structure. Note that, at $q \ll 1$, the magnetic dipole contribution is small, so that the inequality, $Q_1^{(m)} \ll Q_1^{(e)}$, is satisfied at almost all values of parameters except those regions close to the anapole conditions. The closed singular line in figure 2*b* corresponds to zero energy flow. In the vicinity of this singular line, the Poynting vector produces vortices, as illustrated in figure 2*c*, which are similar to those observed in the scattering from small plasmonic particles [16,33].

Another way to visualize the toroidal symmetry of the mode is by plotting the electric and magnetic field distributions inside the particle in mutually perpendicular planes, as shown in

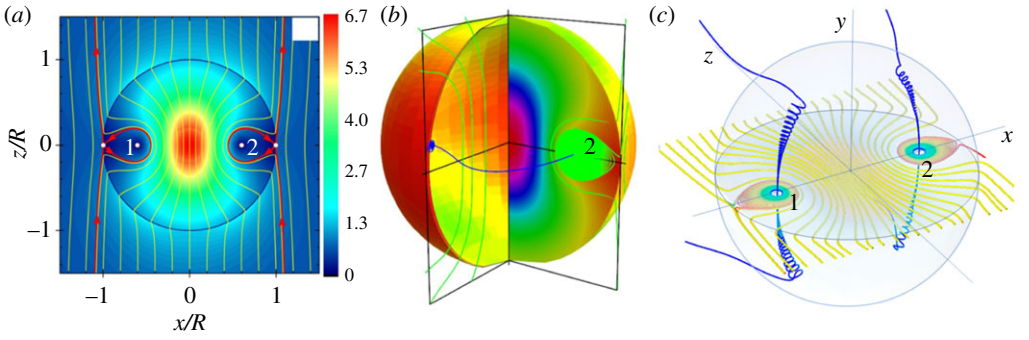

Figure 2. (*a*) Two-dimensional Poynting vector in the $\{x, z\}$-plane for $q = 0.3$ and $n = 15.0116$. Colour panel presents the variation in the modulus of the Poynting vector. The full number of modes in the Mie theory is taken into account. There are two saddles and two focal points. The red lines show the separatrices. Inside the particle, one can see the loops of separatrices representing the cross sections of the electric toroidal dipole. (*b*) Three-dimensional Poynting vector distribution. The focal points in figure 2 are, in reality, unstable saddle–focal points. Through these points goes the closed singular line, which provides the axis of the toroidal mode. A one-quarter part of this line is shown by the blue line. The green lines show the untwisted spiral of the Poynting vector in the $\{x, z\}$-plane. (*c*) Vortices around the closed singular line, which provides the axis for the toroidal mode.

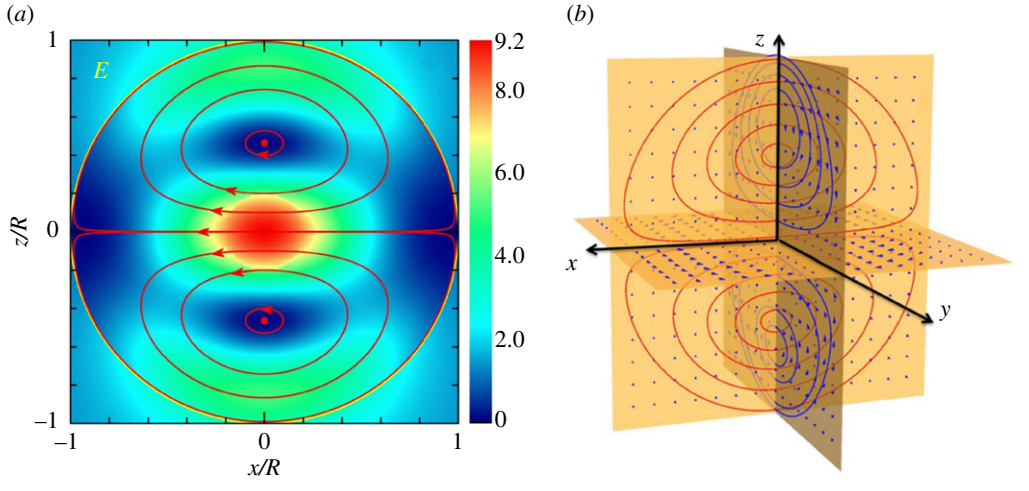

Figure 3. (*a*) Distribution of the electric vector **E** within the $\{x, z\}$-plane through the particle diameter. Colour panel indicates the value of the electric intensity $\mathbf{E}^2$ in this plane. (*b*) Three-dimensional distributions of electric **E** (red lines) and magnetic **H** (blue lines) vectors within the planes through the particle diameter.

figure 3. Here, the electric field is shown in the $\{x, z\}$-plane passing through the diameter of the particle in figure 3*a*, with the colour map representing the intensity $\mathbf{E}^2$ distribution. The corresponding magnetic field lines are represented in the perpendicular $\{y, z\}$-plane in figure 3*b*, clearly revealing the poloidal displacement current distribution, associated with the toroidal dipole mode [32]. Performing a Cartesian multi-pole expansion of the induced displacement current reveals the dominant contributions of the electric and toroidal dipole moments (not shown here) [31]. Thus, one can conclude that the Fano resonance observed is related to the constructive and destructive interference of the electric dipole and toroidal dipole moments.

As shown in figure 1*b* the corresponding Fano resonance arises in the vicinity of the zero of the electric dipole mode, $a_1 = 0$. This condition yields the equation

$$1 - n^2 + q(n^2 - 1 + n^2q^2)\cot(q) + nq(n^2 - 1 - n^2q^2)\cot(nq) + nq^2(1 - n^2)\cot(q)\cot(nq) = 0. \quad (3.1)$$

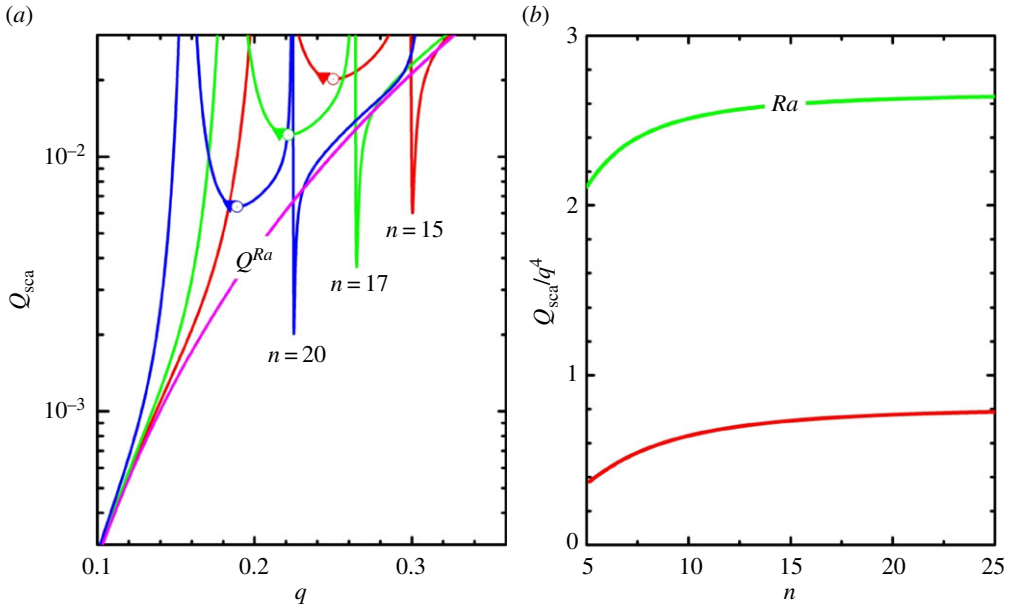

Figure 4. (*a*) Scattering efficiencies versus size parameter for three values of refractive index: $n = 15$ (red), $n = 17$ (green) and $n = 20$ (blue). Open circles present positions of the local minima in scattering. The triangles show the scattering in the points which correspond to minimal forward scattering at the second Kerker condition. (*b*) The dependencies Q_{sca}/q^4 versus refractive index along the Rayleigh scattering (green) and anapole mode (red).

Within the above equation, one should consider $\cos(q) \neq 0$ and $\cos(nq) \neq 0$. For each value of the refractive index, there is an infinite set of solutions with corresponding size parameter q. However, just the first root of (3.1) corresponds to the global minimum of Q_{sca}.

It is important to emphasize that the anapole mode produces the global minimum in scattering efficiency. A minimization of the differential scattering only [34–37] does not minimize the total scattering. For example, a minimization of the forward scattering (the so-called second Kerker condition [34]) is quite close to a local minimum in scattering (figure 4*a*), but it is still larger than the Rayleigh scattering. A better way to visualize the global minimization of the scattering cross section is shown in figure 4*b*. The scattering efficiencies, normalized to the fourth power of the size parameter, Q_{sca}/q^4, are plotted as a function of the refractive index of the particle in the Rayleigh limit and at the minimum associated with the anapole excitation.

Although outside the scope of this work, it must be mentioned that further minimization of the scattering cross section is possible if one considers, for example, spheroidal particles [38].

It is also interesting to note that the behaviour of the directional scattering for a spherical particle near the magnetic dipole resonance and near the anapole mode is quite different. The forward (Q_{FS}) and backward (Q_{BS}) scattering efficiencies for a spherical particle from Mie theory are defined as:

$$\left.\begin{aligned} Q_{FS} &= \frac{1}{q^2}\left|\sum_{\ell=1}^{\infty}(2\ell+1)(a_\ell + b_\ell)\right|^2 \\ \text{and} \quad Q_{BS} &= \frac{1}{q^2}\left|\sum_{\ell=1}^{\infty}(2\ell+1)(-1)^\ell(a_\ell - b_\ell)\right|^2. \end{aligned}\right\} \tag{3.2}$$

While a total suppression of the forward scattering is forbidden by the optical theorem [39], the backscattering of a small particle can be almost completely suppressed when the condition $a_1 = b_1$ (*the first Kerker condition*) is fulfilled. The minimization of the forward to backward ratio is often referred to as the *second Kerker condition* [34]. For a sphere with a size parameter $q = 0.3$

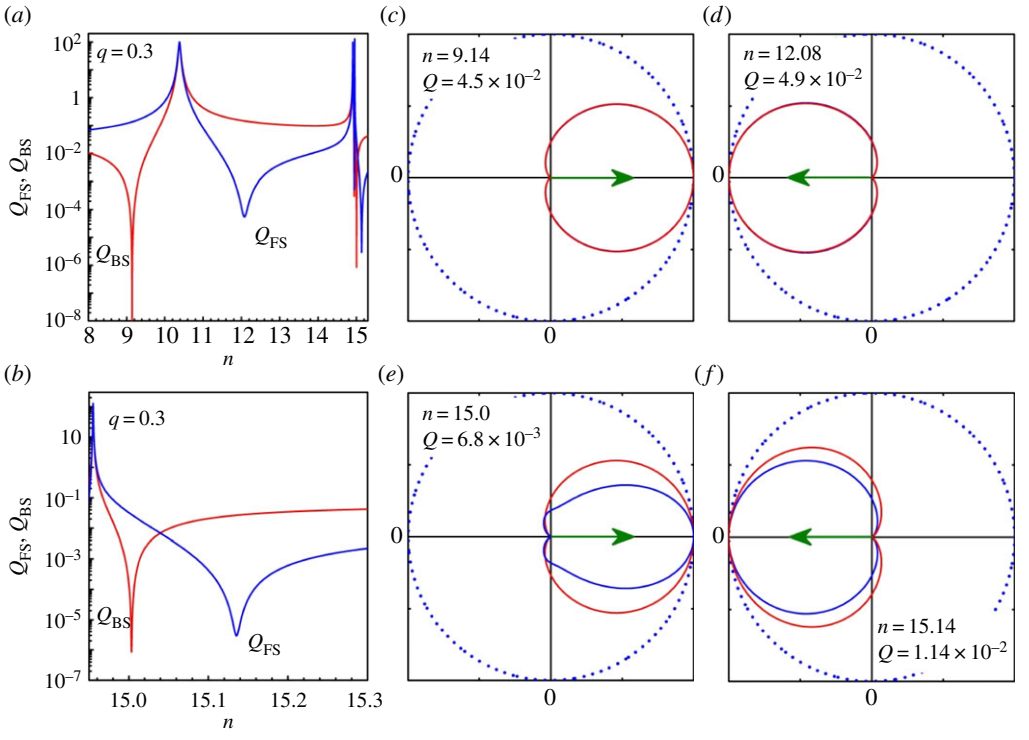

Figure 5. (*a*,*b*) Forward and backward scattering efficiencies for a small particle $q = 0.3$ versus refractive index n. (*c*–*f*) The polar scattering diagrams in the x–z plane (azimuthal angle $\varphi = 0$ in Mie theory) for different refractive index n. Blue lines show linearly polarized light and red lines represent non-polarized light. Arrows indicate the direction of scattering.

the first Kerker condition is met for an index $n \approx 9.14$, while the second is met for $n \approx 12.08$. It is interesting to note that the second branch of solutions for Kerker conditions yields the values $n \approx 14.99$ and $n \approx 15.14$, which are located in the vicinity of the anapole mode. The corresponding polar scattering diagrams [15] are shown in figure 5. The scattering pattern at Kerker's conditions does not depend on the incident polarization, yielding the same results for linearly polarized and unpolarized light (i.e. it has rotational symmetry). By contrast, the scattering pattern near the anapole condition is not rotationally symmetric, thus yielding polarization-dependent scattering patterns (except, of course, in the backward and forward directions). This behaviour is quite similar to the change of directivity in the vicinity of quadrupole resonance within weakly dissipating plasmonic particles [14].

4. Conclusion

We have found conditions for which the scattering of a small spherical dielectric particle, $q \ll 1$, is strictly below the value that follows from the Rayleigh limit. It is related to the excitation of an anapole mode with an associated spectral Fano line-shape. Although similar effects have been found previously for a homogeneous dielectric rod [30], the physics was explained in a different way. It is important to highlight that the presented results refer to a homogeneous, isotropic, small particle. The only conditions for such ultra-small scattering are a small size parameter, $q \ll 1$, a large refractive index, typically $n > 5$, and weak dissipation. There are a number of materials fulfilling these conditions in the far-IR and microwave regions, such as SiC, TiO_2 and ceramics among others [40]. We foresee that clusters of material assembled from such particles may have interesting properties such as high transparency, i.e. the scattering effect in the extinction could be strongly suppressed.

Authors' contributions. B.L. initiated the study of the anapole effect by a small spherical particle. All authors contributed to discussions, writing and editing this paper.

Competing interests. We declare we have no competing interests.

Funding. B.L., R.P.-D. and A.I.K. acknowledge support by DSI core funds and an A*STAR Science and Engineering Research Council (SERC) Pharos grant no. 1527000025. A.E.M. and Y.S.K. were supported by the Australian Research Council.

Acknowledgements. The authors acknowledge Reuben M. Bakker for manuscript edits and proof reading.

References

1. Rayleigh L. 1871 On the light from the sky, its polarization and colour. *Philos. Mag.* **41**, 107–120 274–279.
2. Rayleigh L. 1871 On the scattering of light by small particles. *Philos. Mag.* **41**, 447–454.
3. Ufimtsev PY. 1971 *Method of edge waves in the physical theory of diffraction*. Dayton, OH: U.S. Air Force, Foreign Technology Division.
4. Ufimtsev PY. 2006 *Fundamentals of the physical theory of diffraction*. New York, NY: Wiley.
5. Kerker M, Wang D, Giles G. 1983 Electromagnetic scattering by magnetic spheres. *J. Opt. Soc. Am.* **73**, 765–767. (doi:10.1364/JOSA.73.000765)
6. Chew H, Kerker M. 1976 Abnormally low electromagnetic scattering cross sections. *J. Opt. Soc. Am.* **66**, 445–449. (doi:10.1364/JOSA.66.000445)
7. Kerker M. 1975 Invisible bodies. *J. Opt. Soc. Am.* **65**, 376–379. (doi:10.1364/JOSA.65.000376)
8. Leonhardt U. 2006 Optical conformal mapping. *Science* **312**, 1777–1780. (doi:10.1126/science.1126493)
9. Pendry JB, Schurig D, Smith DR. 2006 *Controlling electromagnetic fields*. *Science* **312**, 1780–1782. (doi:10.1126/science.1125907)
10. Alù A, Engheta N. 2008 Multifrequency optical invisibility cloak with layered plasmonic shells. *Phys. Rev. Lett.* **100**, 113901. (doi:10.1103/PhysRevLett.100.113901)
11. Paniagua-Domínguez R, Abujetas DR, Froufe-Pérez LS, Sáenz JJ, Sánchez-Gil JA. 2013 Broadband telecom transparency of semiconductor-coated metal nanowires: more transparent than glass. *Opt. Express* **21**, 22 076–22 089. (doi:10.1364/OE.21.022076)
12. Chen P-Y, Soric J, Alù A. 2012 Invisibility and cloaking based on scattering cancellation. *Adv. Mater.* **24**, OP281–OP304. (doi:10.1002/adma.201202624)
13. Miroshnichenko AE, Flach S, Kivshar YS. 2010 Fano resonances in nanoscale structures. *Rev. Mod. Phys.* **82**, 2257–2298. (doi:10.1103/RevModPhys.82.2257)
14. Luk'yanchuk B, Zheludev NI, Maier SA, Halas NJ, Nordlander P, Giessen H, Chong CT. 2010 The Fano resonance in plasmonic nanostructures and metamaterials. *Nat. Mater.* **9**, 707–715. (doi:10.1038/nmat2810)
15. Born M, Wolf E. 1999 *Principles of optics*, 7th edn. Cambridge, UK: Cambridge University Press.
16. Wang ZB, Luk'yanchuk BS, Hong MH, Lin Y, Chong TC. 2004 Energy flow around a small particle investigated by classical Mie theory. *Phys. Rev. B* **70**, 035418. (doi:10.1103/PhysRevB.70.035418)
17. Bohren CF. 1983 How can a particle absorb more than the light incident on it? *Am. J. Phys.* **51**, 323–327. (doi:10.1119/1.13262)
18. Tribelsky MI, Luk'yanchuk BS. 2006 Anomalous light scattering by small particles. *Phys. Rev. Lett.* **97**, 263902. (doi:10.1103/PhysRevLett.97.263902)
19. van de Hulst HC. 2005 *Light scattering by small particles*. New York, NY: Dover.
20. Evlyukhin AB, Reinhardt C, Seidel A, Luk'yanchuk B, Chichkov BN. 2010 Optical response features of Si-nanoparticle arrays. *Phys. Rev. B* **82**, 045404. (doi:10.1103/PhysRevB.82.045404)
21. Garcia-Etxarri A, Gomez-Medina R, Froufe-Perez LS, Lopez C, Chantada L, Scheffold F, Aizpurua J, Nieto-Vesperinas M, Sáenz JJ. 2011 Strong magnetic response of submicron silicon particles in the infrared. *Opt. Express* **19**, 4815–4826. (doi:10.1364/OE.19.004815)
22. Kuznetsov AI, Miroshnichenko AE, Fu YH, Zhang JB, Luk'yanchuk B. 2012 Magnetic light. *Sci. Rep.* **2**, 492. (doi:10.1038/srep00492)
23. Evlyukhin AB, Novikov SM, Zywietz U, Eriksen RL, Reinhardt C, Bozhevolnyi SI, Chichkov BN. 2012 Demonstration of magnetic dipole resonances of dielectric nanospheres in the visible region. *Nano Lett.* **12**, 3749–3755. (doi:10.1021/nl301594s)

24. López-Tejeira F, Paniagua-Domínguez R, Rodríguez-Oliveros R, Sánchez-Gil JA. 2012 Fano-like interference of plasmon resonances at a single rod-shaped nanoantenna. *New J. Phys.* **14**, 023035. (doi:10.1088/1367-2630/14/2/023035)
25. Verellen N, López-Tejeira F, Paniagua-Domínguez R, Vercruysse D, Denkova D, Lagae L, Van Dorpe P, Moshchalkov VV, Sánchez-Gil JA. 2014 Mode parity-controlled Fano- and Lorentz-like line shapes arising in plasmonic nanorods. *Nano Lett.* **14**, 2322–2329. (doi:10.1021/nl404670x)
26. Fan P, Yu Z, Fan S, Brongersma ML. 2014 Optical Fano resonance of an individual semiconductor nanostructure. *Nat. Mater.* **13**, 471–475. (doi:10.1038/nmat3927)
27. Poddubny AN, Rybin MV, Limonov MF, Kivshar YS. 2012 Fano interference governs wave transport in disordered systems. *Nat. Commun.* **3**, 914. (doi:10.1038/ncomms1924)
28. Rybin MV, Sinev IS, Samusev KB, Miroshnichenko AE, Kivshar YS, Limonov MF. 2014 Fano resonances in high-index dielectric photonic structures. *Proc. SPIE* **9127**, 912712. (doi:10.1117/12.2051945)
29. Tribelsky MI, Miroshnichenko AE. 2016 Giant in-particle field concentration and Fano resonances at light scattering by high-refractive index particles. *Phys. Rev. A* **93**, 053837. (doi:10.1103/PhysRevA.93.053837)
30. Rybin MV, Filonov DS, Belov PA, Kivshar YS, Limonov MP. 2015 Switching from visibility to invisibility via Fano resonances. Theory and experiment. *Sci. Rep.* **5**, 8774. (doi:10.1038/srep08774)
31. Miroshnichenko AE, Evlyukhin AB, Yu YF, Bakker RM, Chipouline A, Kuznetsov AI, Luk'yanchuk B, Chichkov BN, Kivshar YS. 2015 Nonradiating anapole modes in dielectric nanoparticles. *Nat. Commun.* **6**, 8069. (doi:10.1038/ncomms9069)
32. Papasimakis N, Fedotov VA, Savinov V, Raybould TA, Zheludev NI. 2016 Electromagnetic toroidal excitations in matter and free space. *Nat. Mater.* **15**, 263. (doi:10.1038/nmat4563)
33. Luk'yanchuk BS, Miroshnichenko AE, Kivshar YS. 2013 Fano resonances and topological optics: the interplay of far- and near-field interference phenomena. *J. Opt.* **15**, 073001. (doi:10.1088/2040-8978/15/7/073001)
34. García-Cámara B, Saiz JM, González F, Moreno F. 2010 Nanoparticles with unconventional scattering properties: size effects. *Opt. Commun.* **283**, 490–496. (doi:10.1016/j.optcom.2009.10.027)
35. Geffrin JM *et al.* 2012 Magnetic and electric coherence in forward- and back-scattered electromagnetic waves by a single dielectric subwavelength sphere. *Nat. Commun.* **3**, 1171. (doi:10.1038/ncomms2167)
36. Fu YH, Kuznetsov AI, Miroshnichenko AE, Yu YF, Luk'yanchuk B. 2013 Directional visible light scattering by silicon nanoparticles. *Nat. Commmun.* **4**, 1527. (doi:10.1038/ncomms2538)
37. Person S, Jain M, Lapin Z, Sáenz JJ, Wicks G, Novotny L. 2013 Demonstration of zero optical backscattering from single nanoparticles. *Nano Lett.* **13**, 1367–1868. (doi:10.1021/nl4005018)
38. Luk'yanchuk B, Voshchinnikov N, Paniagua-Dominguez R, Kuznetsov A. 2015 Optimum forward light scattering by spherical and spheroidal dielectric nanoparticles with high refractive index. *ACS Photonics* **2**, 993–999. (doi:10.1021/acsphotonics.5b00261)
39. Alù A, Engheta N. 2010 How does zero forward scattering in magnetodielectric nanoparticles comply with the optical theorem? *J. Nanophotonics* **4**, 041590. (doi:10.1117/1.3449103)
40. Palik ED. 1985 *Handbook of optical constants of solids*. New York, NY: Academic.